The X-point radiation regime in detached H-Modes in full-tungsten ASDEX Upgrade

F. Reimold[1], M. Bernert[2], A. Kallenbach[2], B. Lipschultz[3], G. Meisl[2], S. Potzel[2], M.L. Reinke[3], M. Wischmeier[2], D. Wünderlich[2], the EUROfusion MST1 team* and the ASDEX Upgrade team

[1]*Forschungszentrum Jülich, IEK-4, 52425 Jülich, Germany*

[2]*Max Planck Institute for Plasma Physics, 85748 Garching, Germany*

[3]*University of York, York Plasma Institute, Heslington, York, United Kingdom YO1 9DD*

Introduction

Operation with a detached divertor is mandatory in future fusion devices, such as ITER and DEMO, in order to reconcile the large power fluxes into the divertor with the heat load and erosion limits of the divertor target. In ASDEX Upgrade (AUG) H-Mode discharges additional seeding of impurities has been necessary to dissipate the power in the Scrape-Off Layer (SOL) by radiation losses to achieve complete detachment with larger heating power (P_H). In standard operation of AUG at plasma currents above $I_P = 0.8$ MA, the vertical inner divertor target is usually detached. Partial detachment at the outer strike-point with a strong drop of plasma pressure along field lines and an ion flux reduction can be obtained with impurity seeding. In order to detach the outer target completely [1], a transition into an X-point radiation regime, which is characterized by intense, localized radiation at the X-point inside the confined plasma, seems to be required at AUG. Similar transitions have also been observed in JET [2], DIII-D [4] and JT-60U [6]. With a carbon first-wall such a transition was generally avoided as the radiation at the X-point was an unstable operational scenario. Recent observations [1, 2] and SOLPS modeling [3] have shown that in an all-metal machine such as AUG and JET the X-point radiation regime can be stable, controllable and reversible. In JET the X-point radiation regime has been observed for a number of impurities such as N, Ne and Ar [2]. In AUG high radiation scenarios with detachment of various degree have been developed for N, Ar and Kr [1, 5, 7]. With nitrogen seeding a transition into an X-point radiation regime occurs that is beneficial for power exhaust.

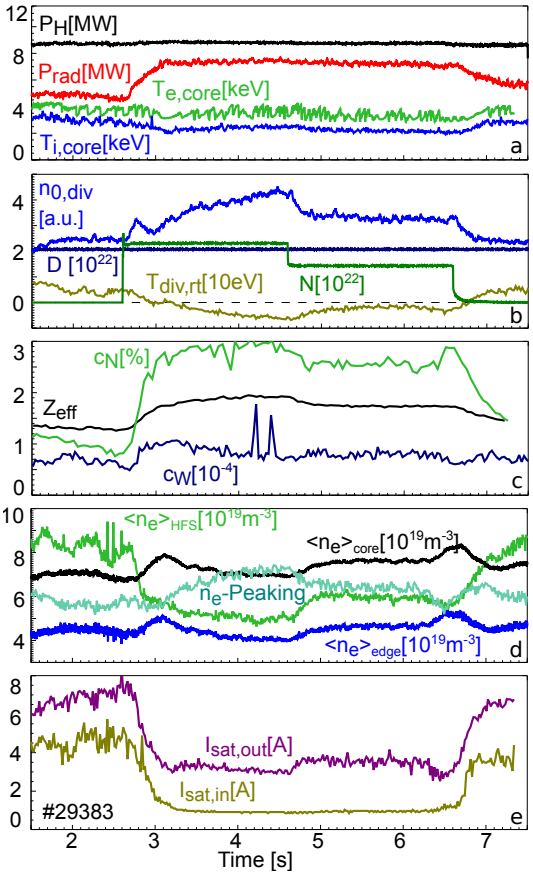

Figure 1: *Discharge overview for #29383.*

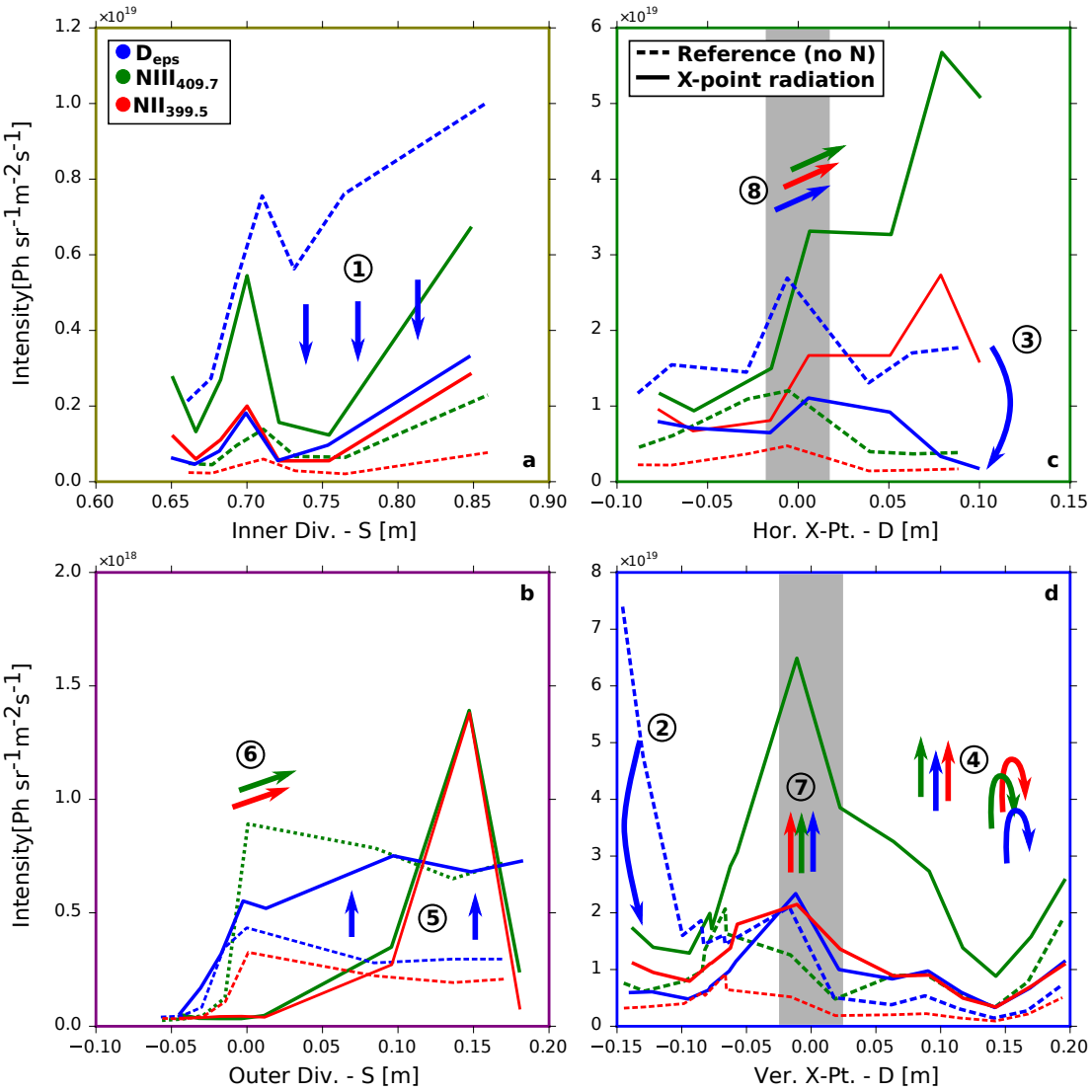

Figure 2: *Line integrated line intensities for the spectroscopic lines of sight (Fig. 3) along the inner (a) and outer (b) divertor target as well as the horizontal (c) and vertical (d) views across the X-point are shown for Balmer, NII, NIII as dashed lines for a reference before N-seeding and as solid lines during the X-point radiation regime. The grey shaded regions indicate the uncertainty of the X-point coordinates. The arrows and numbers indicate the sequence of the intensity profiles evolution.*

Observation of the X-point radiation regime

Stable H-mode operation at power levels of $P_H/R = 3$–$12\,MW/m$ at $H_{98} > 0.85$ with $I_P = 0.8$–$1.2\,MA$ and with both targets detached has been demonstrated in the all-tungsten tokamak AUG [1]. Empirically, complete detachment coincides with the observation of stable, strongly localized and intense radiation inside the confined region at the X-point. This X-point radiation regime has been observed with the application of intense nitrogen seeding in AUG H-Modes ($\Gamma_N \sim 10^{22}\,e^-/s$). With the transition into the X-point radiation regime the divertor plasma changes and complete detachment in H-Mode discharges can be achieved even with high heating power ($> 10\,MW$). SOLPS5.0 simulations indicate that the power dispersal within the confined plasma by the intense X-point radiation starves the divertor of power [8]. In conjunction with an increased radial transport in the divertor, the simulations show that the experimental

*See http://www.euro-fusionscipub.org/mst1.

reduction of the power loads as well as the level of recycling fluxes that can be sustained at the divertor plate are reproduced [3].

Timetraces of a discharge with medium heating power ($P_H = 8.5$ MW) that exhibits the X-point radiation regime for $t > 3.2$ s and with completely detached targets for $4.0\,\text{s} < t < 4.5\,\text{s}$ are shown in Fig. 1. In order to analyze the effect of the X-point radiation on the radiation pattern in the divertor and at the X-point the, line intensities of a Balmer (D_ε - 396.9 nm), a NIII ($2s^2 2p(3s-3p)$ - 409.7 nm) and a NII ($2s^2(3s-3p)$ - 399.5 nm) transition are plotted in Fig. 2. The intensity profiles for the inner (a) and outer (b) divertor as well as for the horizontal (c) and vertical (d) lines of sight across the X-point as shown in Fig. 3 are plotted for a reference time before nitrogen seeding without X-point radiation (2.6 s) and during the X-point radiation phase with intense nitrogen seeding (4.5 s).

A detailed description of the sequence of detachment that is triggered by the impurity radiation can be found in Ref. [1]. A high-field side high density (HFSHD) in the inner divertor as described in Ref. [9] is reduced within 200 ms of the application of the nitrogen seeding (Fig. 1.d). This coincides with an initial density increase by about 15 % [1, 7]. The collapse of the HFSHD is reflected in a strong decrease of the Balmer radiation in far SOL at and close to the inner target by more than an order of magnitude ((1-3) in Fig. 2). It can also be observed in the electron densities derived from Stark broadening. The formation of the X-point radiation takes place in about 500 ms after the application of nitrogen seeding. The radiated power fraction (f_{rad}) increases from about 55 to 80 %. In Fig. 4, the time evolution of the Balmer intensity seen by the horizontal views above the X-point is shown. The increased power losses lead to an initial drop of the Balmer intensity (black arrow) due to the collapse of the HFSHD in the inner divertor, that is followed by a slower evolution of the X-point radiation over the next 1.5 s, which leads to a further increase of f_{rad} to 85 %. During this evolution the nitrogen line intensities at the outer divertor first increase, then roll-over and move out from the strikepoint into the far SOL (4+6 in Fig. 2). The reduction in the initially dominant NIII line is stronger than in the NII line. Consistent with the drop of the realtime divertor target temperature signal $T_{div,rt}$ in Fig. 1.b, both are indicators of a temperature drop in the outer divertor that shifts the ionization balance towards lower ionization stages. In line with Langmuir probes and Stark broadening measurements of an increased density in the outer divertor, the Balmer line intensities increase along the whole outer target (4+5 in Fig. 2) with seeding. At the same time, the outer divertor volume shows a strong increase of the nitrogen and Balmer line radiation that is most pronounced in the X-point region (7-8 in Fig. 2). The stronger increase of radiation in the horizontal views across the X-point also suggest that the radiation region is poloidally elongated along the fluxsurface.

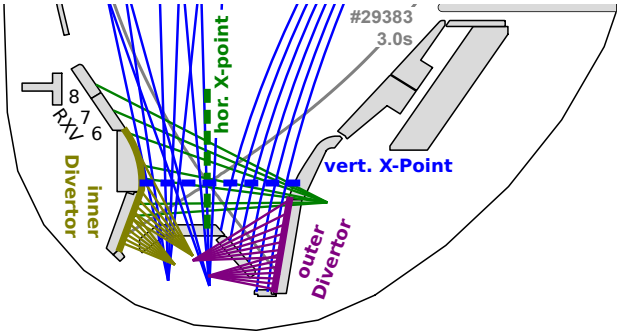

Figure 3: *Line of sight geometry and reference planes are shown.*

As shown in Fig. 4, Balmer radiation also emerges in the confined plasma above the X-point after 3.1 s and keeps increasing by factor of 2–10 during the further evolution. At the same time, the line integrated core density decreases again and the previous increase is almost reversed. At

about 4.0 s (dotted line in Fig. 4), the coincident increase of Balmer radiation in RXV7 and the drop of nitrogen radiation in RXV6 indicates a slow upward motion of the radiation layers. A radial extent of a region with temperatures below 5 eV of about 5 cm can be estimated from the separation of the lines of sight and the change in the relative intensities of Balmer and nitrogen radiation.

The existence of low temperatures of the order of 1 eV close to the X-point is also suggested by measurements of the Balmer line intensity ratio D_ε/D_δ. Fig. 4.b shows that the line ratio close to the X-point attains values that imply a dominantly recombining plasma before the seeding is reduced (blue arrow). However, it has to be noted that the interpretation of line intensity ratios from line-integrated measurements in non-uniform plasmas is challenging and verification of this first indications are necessary.

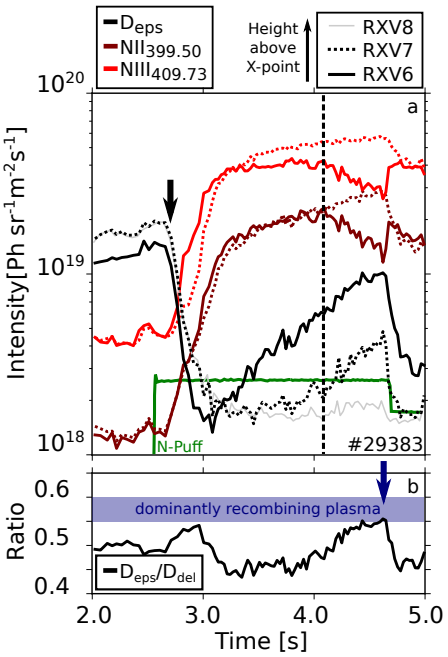

Figure 4: *Time evolution of line intensities (a) and Balmer (b) line intensity ratios for horizontal lines of sight above the X-point (see Fig. 3).*

Summary & Outlook

In summary, it has been shown that the X-point radiation regime is a stable operational scenario with completely detached targets that features intense, localized radiation at the X-point inside the confined plasma. In the presented feed-forward seeding scheme, the X-point radiation shows a slow radial inward motion that leads to the formation of a dense, low temperature region at the X-point with a possibly recombining plasma.

Similar analysis including data for higher charge states of impurity line radiation need further development of the analysis tools and will be addressed in the future. Forward calculations using validated plasma simulations from codes such as SOLPS combined with collisional radiative models will be used to analyze the line ratios in order to prove or falsify the suggestion of a low temperature, recombining plasma at the X-point. The X-point radiation regime with Ne as a seed impurity as well as the stability and stationarity of the regime will be further investigated.

Acknowledgements

This work has been carried out within the framework of the EUROfusion Consortium and has received funding from the Euratom research and training programme 2014-2018 under grant agreement No 633053. The views and opinions expressed herein do not necessarily reflect those of the European Commission.

References

[1] F. Reimold, et al., Nucl. Fusion 55, (2015) 033004
[2] M. Wischmeier, et al., 25th FEC (IAEA), St. Petersburg (2014)
[3] F. Reimold, et al., Journal of Nuc. Mat. (2015) 0022-3115
[4] T. W. Petrie, et al., Journal of Nuc. Mat. 241-243:639-644 (1997)
[5] M. Bernert, et al., this conference
[6] T. Ishijima, et al., Plasma Phys. Control. Fusion 41 (1999) 1155-1666
[7] A.Kallenbach, et al., Nucl. Fusion 55 (2015) 053026
[8] B. Lipschultz, et al., Journal of Nuc. Mat. 266-269 (1999) 370-375
[9] S. Potzel, et al., Journal of Nuc. Mat. (2015)